Reactive Diffusion between Ultra High Purity Iron and Silicon Wafer

Toshitada Shimozaki[1], Akira Hirai[2, *], Takahisa Okino[3] and Chan-Gyu Lee[4]

[1] *The Center for Instrumental Analysis, Kyushu Institute of Technology, Tobata Kitakyushu 804-8550, Japan*
[2] *Department of Materials Science and Engineering, Faculty of Engineering, Kyushu Institute of Technology, Tobata Kitakyushu 804-8550, Japan*
[3] *College of Liberal Arts and Sciences, Nippon Bunri University, Oita 870-0316, Japan*
[4] *Department of Materials Science and Engineering, Changwon National University, Changwon, Kyungnam, 541-773, Korea*

Reactive diffusion between iron and silicon wafer has been studied by using 99.995% electrolytic iron flakes (4.5N–Fe), a 99.5% iron sheet (3N–Fe) and two kinds of iron plates having different oxygen contents which were made by melting the same 99.9% electrolytic iron flakes under different conditions. The growth rate of the Fe_3Si diffusion layers formed in the 4.5N–Fe/Si diffusion couples is faster than that in other couples. The authors have previously reported briefly that Fe_3Si formed in bulk Fe/Si diffusion couples consisted of interstitial free iron (IF-steel) and Si wafer grows considerably faster than that in bulk 99.99%Fe (4N–Fe)/Si diffusion couples and proposed a possible explanation that oxygen atoms which initially distribute randomly in the 4N–Fe specimens are enriched in the iron near the Fe/Fe_3Si interface and they react with Si atoms and form SiO_2 film on the surface of voids formed in the iron near Fe/Fe_3Si interface. The SiO_2 film acts as a diffusion barrier and slows down the growth rate of iron silicides. Ti and Al atoms in IF-steel remove the effect of oxygen by scavenging oxygen atoms around them. So, Fe_3Si in the IF-steel/Si couple can grow faster than that in the 4N–Fe/Si couples. This explanation suggests that the growth rate of Fe_3Si is very fast in a Fe/Si diffusion couple, oxygen concentration in the iron is extremely small. The present experimental result that the growth rate of Fe_3Si is faster than the IF-steel/Si diffusion couples supports this explanation because the oxygen concentration in 4.5N–Fe is very small.

1. Introduction

It has been well known that a very small amount of impurities can sometimes change the property of materials drastically. One of the most important effects has been maintained by an addition of B into Ni_3Al, *i.e.*, the plasticity of Ni_3Al at high temperature has been improved by the addition of B.[1] Similarly, in the field of diffusion phenomena, a small amount of impurities act very important role. For example, an addition of about 0.1 mass%Al into molten zinc retard the growth of intermetallic compound between molten zinc and steel sheet during galvanic anneal.[2] On the other hand, an addition of Ti into the steel sheet enhances the growth of the intermetallic compound.[3] The trouble of cut off of Al wire in IC devices due to electro-migration has been drastically improved by adding about 1 mass%Cu into Al wire.[4]

Recently, the authors have studied the reaction diffusion of the Ti–Si binary system by using various purity of titanium plates, viz., 99.8%, 99.99% or 99.9999%Ti, and a ⟨111⟩ oriented Si wafer and reported that the growth rate of the titanium silicides formed in the Ti/Si diffusion couples shows a marked dependence on the purity of Ti.[5–7] It should be noted, here, that there is a clear difference between the growth rates of titanium silicides formed in the 4N-Ti/Si diffusion couples and that in the 6N-Ti/Si couples.[6,7] According to the previous experimental results, Fe atoms in Ti specimen segregate at grain boundaries in $TiSi_2$ and they slow down the growth rate of the $TiSi_2$ in the diffusion couples.[6,7]

The authors have previously reported briefly a similar dependence of growth rate of iron silicides formed in bulk Fe/Si diffusion couples on the purity of iron sheets,[8] viz., 99.99% iron (4N–Fe) and interstitial free steel (IF steel=99.5%Fe). The growth rate of Fe_3Si formed in IF-steel/Si diffusion couples is about ten times faster than that in 4N–Fe/Si couples. Because about 120 ppm oxygen concentration in the 4N–Fe is relatively higher than 5 ppm in the IF-steel, the authors[8] have proposed a preliminary interpretation for this purity dependence of growth rate as that the oxygen atoms, which initially distribute randomly in iron specimen are gathered near the Fe/Fe_3Si interface, react with Si atoms and form SiO_2 films on the surface of voids which are found in iron specimen near Fe/Fe_3Si interface and they act as diffusion barriers. On the contrary, Ti and Al atoms in IF-steel, which are added for a purpose to scavenge interstitial atoms such as oxygen, nitrogen and carbon, will eliminate the effect of oxygen in 4N–Fe. However, there is another possibility that Ti or Mn in IF-steel themselves enhance the growth rate of Fe_3Si but not eliminate the effect of oxygen. So, in this experiment, the effects of oxygen have been studied in detail by using various kinds of iron sheets, especially high purity electrolytic iron flakes with low concentration of O, Ti and Mn.

2. Experimental Procedure

99.995 mass% electrolytic iron flakes (4.5N–Fe: Toho Zinc Co., LTD) of about 10 mm × 10 mm × 1 mm in size, a 99.5% iron sheet (2N–Fe: purchased from Nilaco) and two kinds of iron sheets were used in this experiment. These two kinds of iron sheets were made by melting 99.9 mass% electrolytic iron flakes (Toho Zinc Co., LTD) in a cold-crucible induction furnace under different melting conditions. One is melted in a highly evacuated atmosphere at 1×10^{-6} Pa by adding carbon

Table 1 Chemical compositions. [ppm]

Element	C	Si	Mn	P	S	Cr	Ni	Cu	Sn	Mg	Al	Ti	Co	Zn	N	O
2N–Fe	250	300	1600	50	150	200	400	300	20	—	—	—	—	—	40	10
3N–Fe–L	0.1	—	<0.1	—	1.4	3	<0.1	2	—	0.9	<1	1	0.8	0.7	27	15
3N–Fe—H	0.6	—	<0.1	—	2.3	<1	<0.1	3	—	0.8	<1	0.3	1.5	0.5	27	49
4N–Fe	14	39	<0.1	—	—	1	14	2	—	—	—	—	—	—	32	124
4.5N–Fe	1.0	1.0	0.01	0.2	1.0	—	—	1	0.2	—	—	—	<0.1	—	1	1
IF-steel	23	140	1600	80	39	—	—	—	—	—	240	550	—	—	170	<5

Other elements 4.5N–Fe As: 0.4, B: 0.09 ppm, IF-steel Nb: 200 ppm

powder for deoxidizing. The other is melted in a purified Ar gas atmosphere. The concentrations of oxygen in these ingots were measured by an oxygen and nitrogen analyzer (LECO TC-136). The values for other elements were measured by use of an inductively coupled radio frequency plasma spectrometer (ICP: SHIMADZU ICPS-8000). The chemical compositions of the 3N–Fe ingots after the melt and those of the 2N–Fe sheet and the 4.5N–Fe flakes are shown in Table 1 together with those for the IF-steel as well as the 4N–Fe used in the previous experiment. The concentration of the gas elements such as O, N and C are not considered in these values of purity of 2N–Fe, and 3N–Fe, 4N–Fe and IF-steel but they are considered in the purity of 4.5N–Fe. In the table, 3N–Fe with high oxygen concentration and that with low oxygen concentration are designated as 3N–Fe–H and 3N–Fe–L, respectively.

The 3N–Fe–H and 3N–Fe–L ingots were rolled and cut to the specimens about 10 mm × 10 mm × 0.5 ~ 1.5 mm in size. The 2N–Fe sheets were also rolled and cut to the same specimen size. The thick specimens were used for the experiment at high temperature for a long anneal period. The 4.5N–Fe flakes have two different surfaces. One is the surface that contacts with Ni cathode during making the electrolytic iron. One is the free surface. The grains near the former surface are fine granular grains and those near the later surface are columnar grains. So, the difference between the growth rates due to difference of grain shape has been studied.

These specimens thus made were not recrystallized to avoid the contamination during the annealing. As it has been shown,[7] in the reaction diffusion study of Ti/Si binary system, any differences between the growth of silicides formed in a recrystallized Ti/Si couple and a non-recrystallized Ti/Si diffusion couple have not been found. A ⟨100⟩ oriented, 12.4 mm diameter, 0.6 mm thickness silicon wafer was cut to the same size as the iron specimens. The contact surfaces of Si and Fe specimens were ground on abrasive papers and polished metallographically on a buff with fine alumina powder.

The Fe/Si diffusion couple was annealed under a load of about 0.5 MPa during the annealing by using an air compressor to keep good contact at the interface. The Fe and Si specimens were put on a flat surface of a stainless steel rod. Mica sheets were inserted between the stainless steel rod surfaces and the specimens to prevent the reaction between them. The silicon specimen often separates from the diffusion couple at silicide/silicon interface after the diffusion anneal. Although the reason is not clear whether the volume change effect during diffusion anneal and cooling and/or void formation due to the Kirkendall effect is important. However, it was expected

that a good contact between Fe and silicon surfaces be kept during the annealing because the growth of silicides satisfies the parabolic law. The annealing is performed in an evacuated furnace at a pressure of about 2×10^{-3} Pa at 1193 K for various periods of heating time. It takes about 1.8 ks for heating from $0.9T_{set}$ to T_{set} and 0.9 ks for cooling from T_{set} to $0.9T_{set}$ where T_{set} is the set temperature. This period about 2.7 ks was corrected. However, The periods during the temperature rises up to $0.9T_{set}$ from room temperature and cools down from $0.9T_{set}$ to room temperature were neglected.

After the heating the couple was removed and mounted in a resin. The cross section of the diffusion zone was polished metallographically and analyzed by an electron probe micro analyzer (EPMA: JEOL JCXA 733).

3. Results

3.1 Growth behavior of iron silicides

Relationships between total widths of diffusion layers formed in the 4.5N–Fe/Si, 2N–Fe/Si and 3N–Fe/Si diffusion couples and square root of anneal times are shown in Fig. 1 together with the previous data for IF-steel/Si and 4N–Fe/Si diffusion couples. The widths of Fe_5Si_3, $FeSi$ and $FeSi_2$ are neglected in this figure to avoid complication. In Fig. 1, 4.5N–Fe–C and 4.5N–Fe–F mean that the contact or free surface of the iron specimen is contacted with a silicon surface. Any clear difference between the growth rates of diffusion layers formed in the 4.5N–Fe–C/Si and 4.5N–Fe–F/Si diffusion couples could not be detected. The growth rate of the diffusion layers formed in the 4.5N–Fe/Si diffusion couples is the fastest and is more than ten times faster than that formed in the 3N–Fe–H/Si and the 3N–Fe–L/Si couples. The rate in 2N–Fe/Si diffusion couples is also faster than that in the 3N–Fe–H/Si and the 3N–Fe–L/Si couples but about two times slower than that in the 4.5N–Fe/Si couples. Not only the kinds of diffusion layers formed in the 4.5N–Fe/Si diffusion couples but also their growth rates are similar to that in the IF-steel/Si couples, reported previously. On the other hand the kinds of diffusion layers in the 3N–Fe–H couples are similar to those in the 4N–Fe/Si couples. The ratios of thickness of Fe_3Si to the total thickness of diffusion layers in the 4.5N–Fe/Si and 2N–Fe/Si couples are more than 0.9 and is larger than the ratio of 0.8 for 3N–Fe–L/Si and 0.33 for the 4N–Fe/Si couples.

The growth behavior of total width of diffusion layers for the 4.5N–Fe/Si, 2N–Fe/Si diffusion couples and 4N–Fe–L/Si couples are represented by linear lines which pass the original point, $t = 0$ and $W = 0$. However, the line for the total width of diffusion layers in the 3N–Fe–L/Si diffusion couples
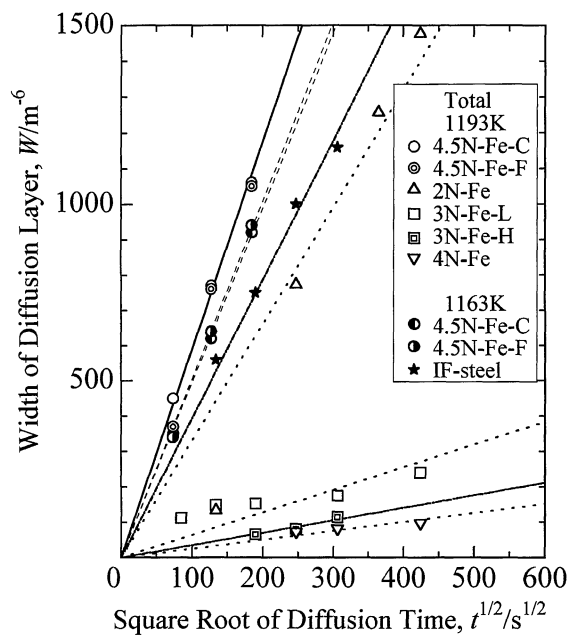
Fig. 1 Relationships between total width of diffusion phase layers in various kinds of diffusion couples and square root of diffusion times at 1163 K and 1193 K.
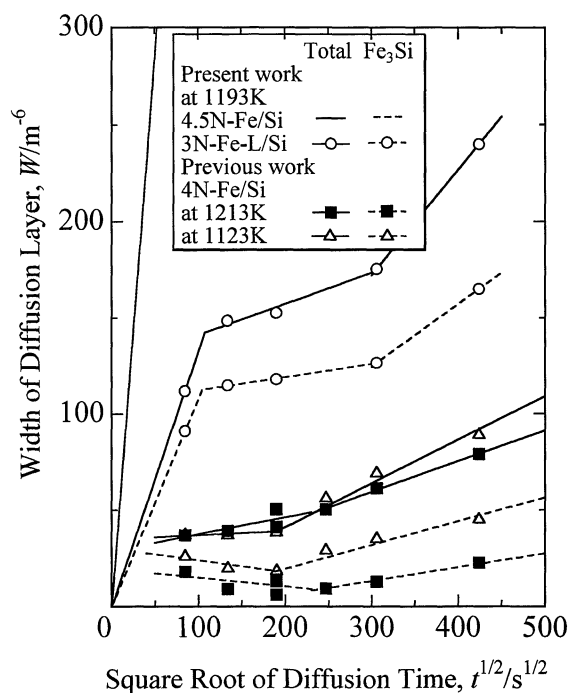

Fig. 2 Relationships between width of Fe_3Si and total width of diffusion layers formed in 3N–Fe–L/Si and 4N–Fe/Si diffusion couples and square root of diffusion times at 1123, 1193 and 1213 K.

Fig. 3 Typical X-ray intensity-distance curves for 4.5N–Fe/Si and 3N–Fe–L/Si diffusion couples.

does not pass the original point. To check this growth behavior, an enlargement of Fig. 1 is shown in Fig. 2. In Fig. 2, the growth of Fe_3Si shows three stages. At first stage, Fe_3Si grows rapidly. At second stage, total width of diffusion layer is kept to be constant. At third stage, Fe_3Si again begins to grow. These stages are also found not only in this diffusion couples at other temperatures but also in the other diffusion couples. For example, the growth behavior of diffusion layers in 4N–Fe/Si diffusion couples at 1123 and 1193 K are shown
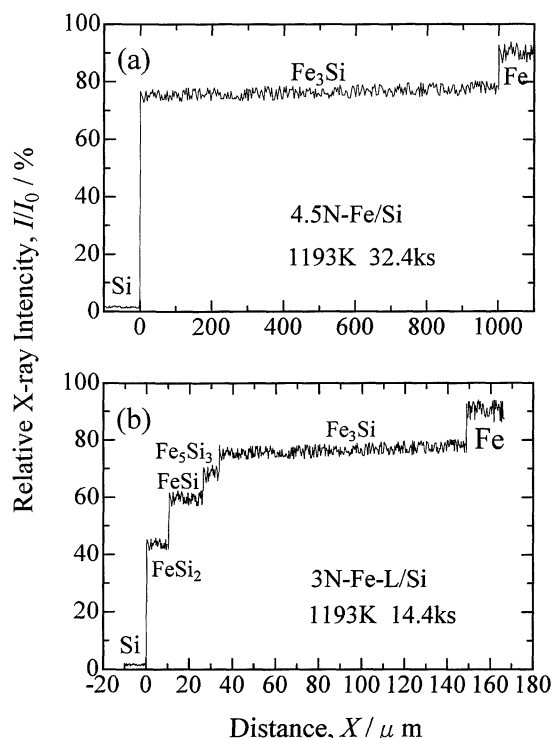
in Fig. 2. The width of Fe_3Si in these couples decreases at stage 2 while the total width is almost kept constantly. In Fig. 2, the growth of Fe_3Si formed in 4N–Fe/Si diffusion couple at 1193 K is also represented as a line that does not pass the original point. The reason for the appearance of these stages will be discussed later.

Although the growth rates of the diffusion layers formed in the 3N–Fe–H, 3N–Fe–L and 4N–Fe/Si diffusion couples are much slower than that in the 4.5N–Fe/Si, 2N–Fe/Si and IF-steel/Si couples, the growth rate of the total width of layers is faster the lower the oxygen concentration of iron among these diffusion couples.

3.2 Interdiffusion coefficients

A $Fe_{K\alpha}X$ ray intensity-distance curve obtained by the EPMA line analysis is shown in Fig. 3(a) for 4.5N–Fe/Si diffusion couple annealed at 1193 K for 32.4 ks and Fig. 3(b) for 3N–Fe–L/Si diffusion couple annealed at 1193 K for 14.4 ks. The concentrations of the diffusion phase layers were determined by the ZAF method. In the 3N–Fe–L/Si diffusion couples, $FeSi_2$, $FeSi$, Fe_5Si_3 and Fe_3Si phases are formed. According to the Fe–Si binary phase diagram,[9] γ solid solution, α-Fe, α_2 and α_1 phases exist in the concentration range $0 \sim 1.5$ at%Si, $2 \sim 14$ at%Si, $14 \sim 18$ at%, $18 \sim 28$ at%Si, respectively at 1193 K. So, any concentration gaps due to two phases region in the Fe–Si phase diagram is not expected. However, a step which suggests the existence of two phases region from 0 to 23 at%Si in the phase diagram is found in the X ray intensity-distance curves as shown in Figs. 3(a) and (b). These steps in the EPMA charts may be correlated with the existence of a crevice near Fe/Fe_3Si interface although the reason for the formation of such crevice is not clear whether due to the Kirkendall effect or volume change effect. In
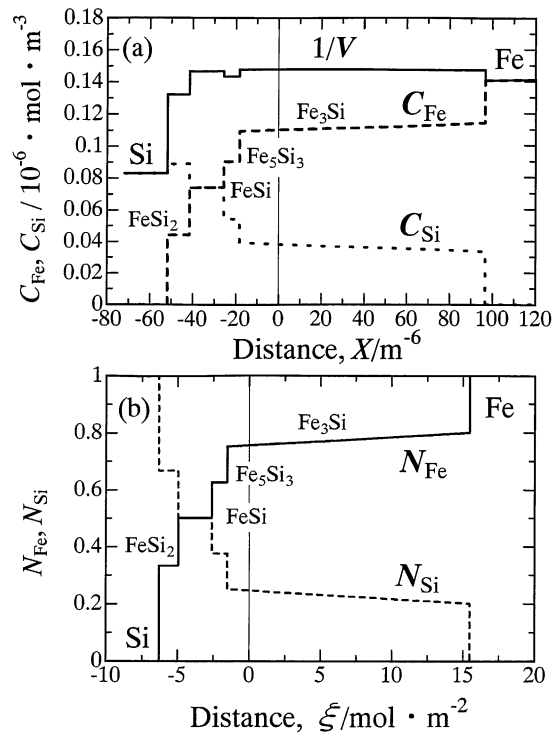
Fig. 4 (a) Mole concentration (C_{Fe}, C_{Si})−Distance(X) Curve and (b) mole fraction (N_{Fe}, N_{Si}) − Distance(ξ) curve in the 3N–Fe–L/Si diffusion couple annealed at 1193 K for 14.4 ks.

Fig. 5 Temperature dependence of various kinds of diffusion coefficients in Fe_3Si and $FeSi_2$.

Table 2 Structure, lattice parameters and molar volumes of iron silicides.

Phase	Crystal type	Lattice parameters (nm)	Number of atoms in unit cell	Molar volume (10^{-6} m³/mol)
Fe	A2	$a = 0.28664$	2	7.089
Fe_3Si	DO_3	$a = 0.5644$	16	6.7645
Fe_5Si_3	$D8_8$	$a = 0.67416$ $c = 0.47079$	16	6.972
FeSi	$B20$	$a = 0.44891$	8	6.807
$\beta FeSi_2$	oC_{48}	$a = 0.9863$ $c = 0.7791$ $c = 0.7833$	48	7.549
Si	A4	$a = 0.54305$	8	12.051

the Fe_3Si phase, Si concentration changes from 22.6 at%Si to 26.4 at%Si, however, no appreciable homogeneity range could be found in the other phases.

The mole concentration of component i (C_i)-distance (X) curve for the 3N–Fe–L/Si diffusion couple is shown in Fig. 4(a) where V is the molar volume of diffusion layers. Between C_i and $1/V$ following relationship holds.

$$1/V = C_1 + C_2$$

The molar volumes, V, were determined with the aid of Pearson's handbooks.[10,11] In Table 2, the crystal structures, lattice parameters and number of atoms in the unit cell, which are required to determine the molar volumes, are shown (The values for molar volume V used here are those at room temperature). It should be noted in Fig. 4(a) that the Si mole concentration (C_{Si})-distance (X) curve shows an irregular concentration reversal at $Si/FeSi_2$ interface while Fe mole con-
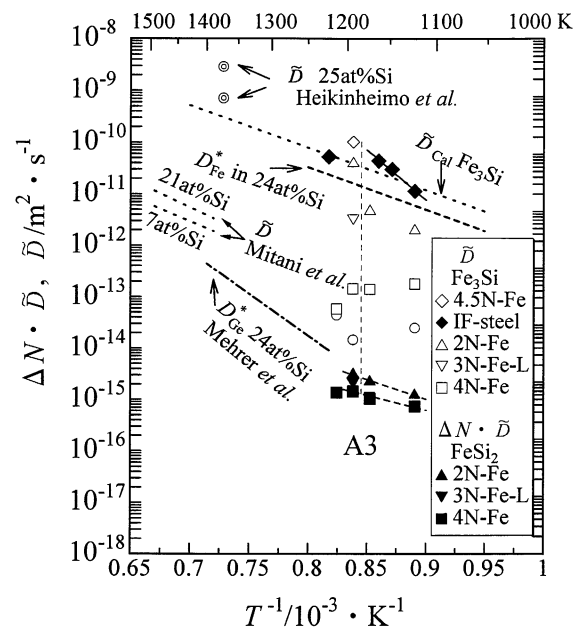
centration (C_{Fe})-distance (X) curve does not. This reversal is attributed to a large molar volume (small $1/V$) of Si. Such concentration reversal is uncommon in binary metallic systems but it often occurs in reaction diffusion between metals and silicon. It seems hard to determine the diffusion coefficients in this system by the Balluffi's equation.[12] Even in this case, a method based on the so called ξ coordinate,[13] i.e., the mole fixed frame of reference, enables us the determination of $\tilde{D}$. The concentration (N_i)-distance (ξ) curve is shown in Fig. 4(b). Here, N_i is the mole fraction of component i. By using this concentration-distance curve, one can calculate the diffusion coefficients with the aid of Matano method.[14]

To determine the interdiffusion coefficients, $\tilde{D}$, the value of concentration gradient in diffusion layers is indispensable. However, the gradient excepting in the Fe_3Si layer could not be detected by the EPMA measurements as described previously. So, $\Delta N \cdot \tilde{D}$ instead of $\tilde{D}$ has been determined for FeSi and $FeSi_2$ phases by Heumann's method[15] taking the volume change effect during diffusion anneal into account. The interdiffusion coefficients of Fe_3Si and $\Delta N \cdot \tilde{D}$ of FeSi and $FeSi_2$ obtained in the previous and the present works are summarized in Fig. 5.

Van Loo et al.[16] have determined the concentration dependence of the interdiffusion coefficients in Fe_3Si by using 99.91%Fe and 99.999 + % polycrystalline Si and shown that $\tilde{D}$ increases with Si concentration up to 25 at% then decreases. Because they have shown two values as $\tilde{D}$ in Fe_3Si, these two values at 25 at%Si are shown in Fig. 5. The temperature dependences of $\tilde{D}$ in Fe_3Si at 7 and 21 at% Si obtained by Mitani et al.[17] are also shown in Fig. 5.

Mehrer et al.[18] have determined the self-diffusion coefficient of Fe, D^*_{Fe}, and the impurity diffusivity of Ge, D^*_{Ge}, in Fe_3Si phase. The diffusivity D^*_{Ge} is expected to be same as D^*_{Ge} in Fe_3Si. These diffusivities at 24 at%Si are also represented in the figure. The diffusivity D^*_{Fe} is more than three orders larger than D^*_{Si}.

van Loo et al.[16] have determined thermodynamics factor, ϕ, in the concentration range from 20 to 30 at%Si at 1373 K to be $3 \sim 7$ ($\phi = 7$ at 25 at%Si) on the base of Lee's[19] thermodynamic data. Because it is expected to be $D_{Si}^* \ll D_{Fe}^*$ in the Fe$_3$Si phase, the well known Manning's equation,[20,21]

$$\tilde{D} = (N_{Fe}D_{Si}^* + N_{Si}D_{Fe}^*)\phi S, \tag{1}$$

can be written as

$$\tilde{D} \simeq N_{Si}D_{Fe}^*\phi S \tag{2}$$

where S is Manning's vacancy flow term[21] and is $1/f_0$ when $D_{Fe}^* \ll D_{Si}^*$ or $D_{Fe}^* \gg D_{Si}^*$. Fe$_3$Si has DO$_3$ structure,[9,10] which based on the bcc structure. The value S for DO$_3$ structure is not well known, so, here, S is assumed to have same value as that for bcc metal, i.e., 1.386. Further, on the assumption that the value ϕ does not depend on temperature, one can calculate $\tilde{D}_{Cal}$ by putting $N_{Si} = 0.25$, $S = 1.386$ and $\phi = 7$ into eq. (2). $\tilde{D}_{Cal}$ thus obtained is shown in Fig. 5 as a dotted line. It coincides well with $\tilde{D}$ for 4.5N–Fe/Si, IF-steel/Si and 2N–Fe/Si diffusion couples rather than those for 3N–Fe–L/Si or 4N–Fe/Si couples.

In the figure, $\Delta N \cdot \tilde{D}$ in FeSi$_2$ for various kinds of diffusion couples are also shown. Although $\Delta N \cdot \tilde{D}$ in FeSi$_2$ does not depend on the purity of Fe, $\tilde{D}$ in Fe$_3$Si is markedly depend on that.

4. Discussions

In the previous paper, our questions were whether the diffusion in IF-steel/Si diffusion couples is enhanced or that in 4N–Fe/Si couples is retarded and what is the element that enhances or retards the diffusion. The present experimental result that the growth rate of Fe$_3$Si layer formed in 4.5N–Fe/Si diffusion couples is faster than that in the IF-steel/Si and 2N–Si diffusion couples and much faster than that in 3N–Fe/Si and 4N–Fe/Si diffusion couples makes these questions clear. The answer is that the diffusion in Fe/Si diffusion couple is essentially very fast as long as highly purified iron is used. However, when an iron sheet that contains some extent of oxygen atoms is used, reaction diffusion between the iron sheet and a silicon wafer is retarded significantly. Ti or Mn atoms eliminate the effects of oxygen but not they enhance the diffusion in Fe/Si diffusion couples themselves. Further, it should be noted hear that only small amount of oxygen atoms of $15 \sim 50$ ppm which exist in the 3N–Fe–L can influence the reaction diffusion between Fe and Si. The present question is why such small amount of oxygen atoms can influence the growth rate so effectively. In the previous paper[8] the authors have found that Ti atoms are enriched at Fe/Fe$_3$Si interface in the IF-steel/Si diffusion couples. This enrichment of Ti may occur due to the movement of the Fe/Fe$_3$Si interface from initial welded position (Matano interface) to that after diffusion anneal, i.e., Ti atoms located randomly in this area are swept up at the interface as illustrated in Fig. 6. We call this effect as sweep up effect due to the movement of interface. In the same manner as Ti atoms, there is a possibility that oxygen atoms are also swept up.

The relationships between the total width of the phase layers or the Fe$_3$Si layer and square root of annealing time shows three stages as it has already shown in Fig. 2. At first stage,
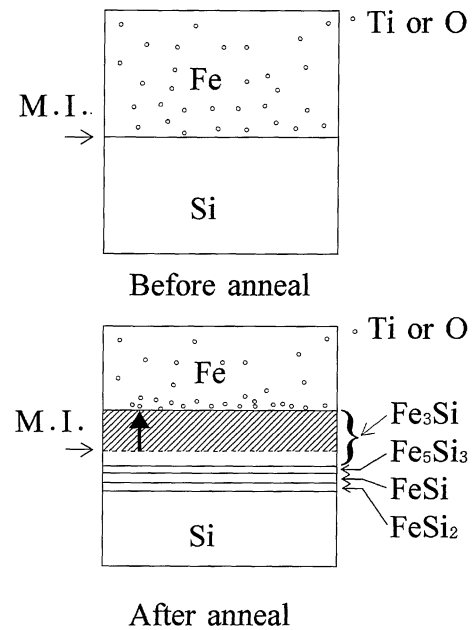

Fig. 6 Illustrations to explain the sweep up effect. Ti or O atoms distribute randomly in iron before anneal. The atoms which distributed in a hatched area are swept up near the Fe/Fe$_3$Si interface due to the movement of the interface after the anneal.

Fe$_3$Si grows rapidly. At second stage, the total width of the diffusion layer is almost kept to be constant. At third stage, Fe$_3$Si again begins to grow slowly in comparison with the first stage. The appearance of these stages can be explained in relation to the behavior oxygen atoms as follow.

In the early stage of diffusion anneal, the oxygen atoms distribute randomly in the Fe plates. Under this condition, diffusion layers can grow fast without any obstructions. After an appropriate extent of movement of Fe/Fe$_3$Si interface from the Matano interface, the oxygen atoms may be swept up and the oxygen concentration in Fe region near the interface reaches to an enough degree of order. Then oxygen atoms begin to react with Si atoms and form SiO$_2$-thin film that retard the diffusion of Fe and Si atoms.

The interdiffusion flux, J_{Fe/Fe_3Si}, of iron in the iron phase at the Fe/Fe$_3$Si interface from the iron phase side to the silicon phase side is defined as

$$J_{Fe/Fe_3Si} = -\frac{\tilde{D}}{V}\frac{\partial N_{Fe}}{\partial X}, \tag{3}$$

by using a definition of the diffusion flux with respect to the mole fixed flame of reference.[22,23] After the formation of SiO$_2$-diffusion barrier, the total amount of interdiffusion flux, J_{Fe/Fe_3Si}, decreases. So, the mass balance at the interface breaks down temporally and the movement of the Fe/Fe$_3$Si interface is retarded. The interdiffusion fluxes of iron at the other interfaces from iron side to silicon side will also gradually decrease and the growth of diffusion layers does not satisfy the parabolic law in the duration that the mass balances at these interfaces break down. Since the mass balances will recover after some periods of anneal time, the diffusion layers begin to grow again satisfying the parabolic law. The growth rate after formation of SiO$_2$ film is of course slower than that before the formation of SiO$_2$. Thus, the appearance of three stages in the growth of diffusion layers in the 3N–Fe–L/Si

diffusion couples and so on can be qualitatively explained in connection with the oxygen behavior in the iron specimens.

In the tracer diffusion experiment done by Mehrer *et al.*, any interfaces are not formed in their specimens. In the inter-diffusion experiment of Fe–Si binary system done by van Loo *et al.* they used diffusion couples in which any interfaces were not formed. Therefore, the swept up effect does not occur in these experiment. This may be the reason for a good agreement of interdiffusion coefficients obtained in this experiment by using 4.5N–Fe and IF-steel, that obtained by van Loo *et al.* and the calculated interdiffusion coefficients that obtained with the aid of Manning's equation by using Mehrer's tracer diffusion coefficients.

From the present experiment another important result has been obtained that the influence due to the contamination or oxidation during diffusion anneal is negligibly small to the growth of diffusion layers in the diffusion couple even in the evacuated atmosphere at about 10^{-3} Pa in this experiment.

The interdiffusion experiment by using the 4.5N–Fe electrolytic iron flaks are now planning. The results will be reported elsewhere.

5. Summary

Reactive diffusion between iron and silicon wafer has been studied by using ultra high purity electrolytic iron flakes of 99.995% and those having different purity and oxygen concentrations. The results have been compared with the previous results obtained by using interstitial free iron and 99.99% iron. The results are summarized as follow.

The growth rate of diffusion layers formed in the ultra high purity electrolytic iron flack/Si diffusion couples was the fastest among these diffusion couples. From this result it has been clarified that

(1)   The growth rate of diffusion layer in Fe/Si diffusion couple is essentially fast.

(2)   The oxygen atoms in iron react with silicon atoms and form SiO_2-film that acts as a diffusion barrier. This thin film slows down the diffusion.

(3)   Ti and Al atoms in the interstitial free iron or Mn in 99.5% iron scavenge oxygen atoms around them and eliminate the effect of oxygen so the growth rate of diffusion layer in these diffusion couple is fast but not they enhance the diffusion.

To explain such effective influence of a small amount of oxygen atoms on the growth rate of diffusion layers, the swept up effect due to movement of interface has been proposed.

REFERENCES

1) G. I. Douglas and W. Dashan: Can. J. Phys. **70** (1992) 860–865.
2) T. Fukuzuka, M. Urai and K. Wakayama: Kobe Steel Eng. Rep. **30** (1980) 77–81.
3) M. Abe, S. Kamihara: Tetsu-to-Hagane **69** (1983) S1061.
4) J. K. Howard and R. F. Ross: Appl. Phys. Letters **18** (1971) 344–349.
5) T. Shimozaki, K. Chikumaru, Y. Wakamatsu and M. Onishi: J. Japan Inst. Met. **60** (1996) 29–36 (in Japanese).
6) T. Shimozaki, T. Okino, M.Yamane, Y. Wakamatsu and M. Onishi: Mater. Trans., JIM **38** (1997) 865–870.
7) T. Shimozaki, T. Okino, M. Yamane and C.-G. Lee: Mater. Trans., JIM **40** (1999) 612–617.
8) T. Shimozaki, A. Hirai, T. Okino and C.-G. Lee: Proceedings of the Fifth International Conference on Diffusion in Materials, DIMAT 2000, Trans Tech Publications Ltd, Zuerich, to be published.
9) Binary Alloy Phase Diagrams, **vol. 2**, ed. by T. B. Massalski *et al.*, (American Society for Metals, Metals Park, Ohio, 1986) pp. 1108.
10) W. B. Pearson: *Handbook of Lattice Spacings and Structures of Metals*, (Pergamon press, London, 1958) pp. 180.
11) P. Villars and L. D. Calvert: *Pearson's Handbook of Crystallographic Data for Intermetallic Phases*, (ASM, Metals Park, Ohio vol. **3**, 1985) pp. 2232.
12) R. W. Balluffi: Acta Metall. **8** (1960) 871–873.
13) M. Cohen, C. Wagner and J.E. Reynolds: Trans. AIME **197** (1953) 1534–1536.
14) C. Matano: Japan J. Physics **8** (1933) 109–113.
15) Th. Heumann: Z. Phys. Chem. **201** (1952) 168–189.
16) E. Heikinheimo, A. A. Kodentsov and F. J. J. van Loo: Scripta Mater. **38** (1998) 1229–1235.
17) H. Mitani, M. Onishi and T. Shikano: J. Japan Inst. Metals. **30** (1966) 141–146.
18) H. Mehrer, M. Eggersmann, A. Gude, M. Salamon and B. Sepiol: Mater. Sci. Eng. **A239–240** (1997) 889–898.
19) B. Lee, S. K. Lee and D. N. Lee: CALPHAD **11** (1985) 253–270.
20) L. S. Darken: Trans. AIME **174** (1948) 184–201.
21) J. R. Manning: *Diffusion kinetics for atoms in crystals*, (Van Nostrand, 1968) Chap. 5.
22) M. Onishi and T. Shimozaki: J. Japan. Inst. Met. **45** (1982) 1–8 (in Japanese).
23) T. Shimozaki, K. Ito and M. Onishi: Trans., JIM **27** (1986) 160–166.